Sborník vědeckých prací Vysoké školy báňské - Technické univerzity Ostrava
číslo 2, rok 2007, ročník LIII, řada strojní
článek č. 1566

BOGDAN SAPIŃSKI*

CONTROL DESIGN FOR AN MR DAMPER IN A DRIVER'S SEAT

NÁVRHU REGULÁTORU PRO MR TLUMIČ SEDADLA ŘIDIČE AUTOMOBILU

Abstract

The paper is concerned with identification and control of the magnetorheological (MR) damper recommended for suspended seat applications. It is assumed that the damper force is given by formula proposed by Spencer and the model exhibits the functional dependence of the parameters on the input current. The identified model is applied in control design for an MR damper in a driver's seat. It is shown that the performance of the feedback system is improved while compared to the open-loop system.

Abstrakt

Příspěvek je zaměřen na identifikaci a řízení magnetorheologických (MR) tlumičů doporučovaných pro aplikace na zavěšených sedačkách. Lze předpokládat, že síla tlumiče je dána vztahem dle Spensera a model dokládá funkční závislost jeho parametrů na vstupním proudu. Identifikovaný model je aplikován v návrhu regulátoru pro MR tlumič sedadla řidiče automobilu. Je ukázáno, že činnost zpětnovazebního systému je zlepšena ve srovnání s otevřenou vazební smyčkou.

1 INTRODUCTION

Control design for a magnetorheological (MR) damper employed in a mechanical system requires a model capable of predicting its behaviour under fluctuating magnetic fields. In the literature we get the model generalization, known as the Spencer model. This model exhibits the functional dependence for the parameters on the input voltage (voltage applied to the damper coil), assuming that the yield stress of the MR fluid is directly dependent on the magnetic field strength. To prove how the model should reproduce an MR damper behaviour its parameters have to be identified. Such identification process for a prototype of an MR damper is described in (Spencer, Dyke et al. 1996).

In the study we used the MR damper of RD-1005-3 series manufactured by Lord Co. which is recommended for suspended seat applications in heavy-duty trucks and off-highway vehicles (http://www.lord.com). We assumed that the damping force is given by formula proposed by Spencer but the model exhibits the functional dependence of the parameters on the input current. For the purpose of identification we conducted a series of the RD-1005-3 tests in which we measured force responses under various displacement excitations and a programmed sequence of input current variations. We determined the model parameters to best fit the experimental data and we showed that the identified model captures the real behaviour throughout the tested range of loading conditions and input current range. Therefore it can be effectively applied in control design. This was illustrated in control design for an MR damper in a driver' seat.

* Department of Process Control, AGH University of Science and Technology, e-mail: deep@agh.edu.pl

2 MR DAMPER: STRUCTURE, OPERATION AND SPECIFICATION

The simplified structure of the RD-1005-3 with main components is shown in Figure 1. The volume of MR fluid portion in the gap, flux guide (piston, ring) and coil create the magnetic circuit (see dash line) in which the magnetic field is produced by the input current.

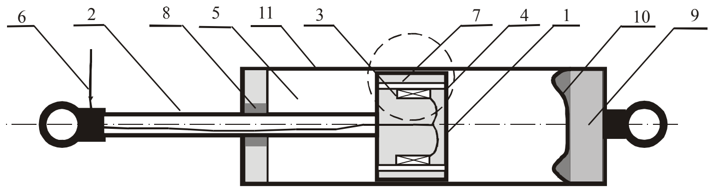

Fig. 1 MR damper structure: 1 – piston head, 2 – piston rod, 3 – coil, 4 – gap, 5 – MR fluid, 6 – wires, 7 – ring, 8 – bearing and seal, 9 – accumulator, 10 – diaphragm, 11 – cylinder

If external forces act on the piston in the absence of a magnetic field, the damping force depends, above all, on the rate of MR fluid flow through the gap, resulting from the pressure differences between the cells. The RD-1005-3 behaves then like a viscous damper. If a magnetic field is applied, the shear stress and the MR fluid viscosity increase the restricting motion of the piston head. As a result, the fluid flow through the gap becomes limited, which produces increased hydraulic resistance to the piston movement and creates a controlled component of the damping force depending on the applied magnetic field.

The RD-1005-3 has: ± 25 mm stroke, extended length 208 mm, compressed length 155 mm, body diameter 41.4 mm and the piston rod diameter 10 mm. An accumulator containing high pressure nitrogen gas compensates changes in the volume of liquid present in chambers. The input voltage is 12 V DC. The input current can be varied between 0 A and 2 A. The coil resistance is 5 Ω at ambient temperature (25°C). The damping forces (peak to peak) are 2224 N (velocity 51×10^{-3} m/s, current 1 A) and 667 N (velocity 200×10^{-3} m/s, current 0 A). Response time (dependent on amplifier type and power supply) is less than 25 ms (time to reach 90% of maximal level during a 0 A to 1 A step input at velocity 51×10^{-3} m/s).

Figure 2 shows typical force-velocity loops of the RD-1005-3. The plots were obtained under sine displacement excitation of 1 Hz, 3×10^{-3} m and constant input currents: 0.0, 0.2, 0.4, 0.8 and 1.0 A.

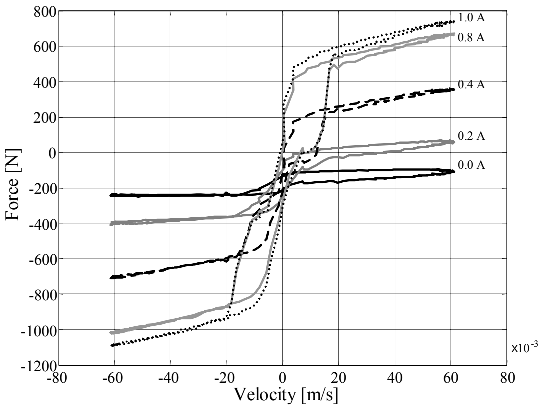

Fig. 2 Force-velocity loops of the damper

3 MODEL OF AN MR DAMPER FOR FLUCTUATING MAGNETIC FIELDS

The Spencer model takes into account visco-plastic and hysteretic rheological behavior of MR fluid (Fig. 3). For the modeling of hysteretic behavior, the model employs a method proposed in (Wen 1976).

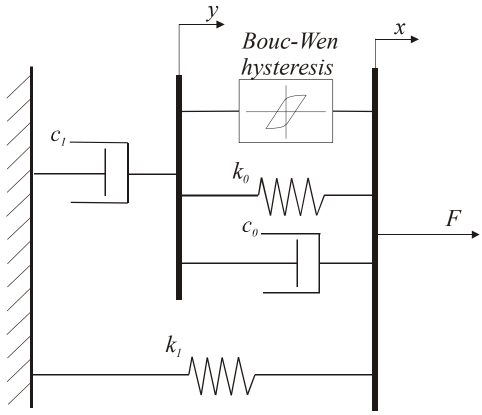

Fig. 3 Spencer model

The damping force of an MR damper is the sum of two components: the component without hysteresis and that defined by an equation associated with the displacement *x* and an evolutional variable z_e, the position of the equation is dependent on whether *n* is an even or odd number (Wen 1976). It was shown that the prediction accuracy is satisfactory for $n = 2$.

Accordingly, the force in the Spencer model for magnetostatic fields is given by:

$$F = \alpha z_e + c_0(\dot{x} - \dot{y}) + k_0(x - y) + k_1(x - x_0) \tag{1}$$

or can be also written as:

$$F = c_1\dot{y} + k_1(x - x_0) \tag{2}$$

The displacement z_e and the displacement *y* are governed by the following equations:

$$\dot{z}_e = -\gamma\left|\dot{x} - \dot{y}\right| z_e\left|z_e\right|^{n-1} - \beta(\dot{x} - \dot{y})\left|z_e\right|^n + A(\dot{x} - \dot{y}) \tag{3}$$

$$\dot{y} = \frac{1}{(c_0 + c_1)}\left[\alpha z_e + c_0\dot{x} + k_0(x - y)\right] \tag{4}$$

where:

β, γ, A	–	determinants of linearity in unloading conditions and smoothness of transition from the pre-yield to post-yield regime of MR fluid,
α	–	stiffness coefficient for the force component associated with z_e,
c_0	–	viscous damping coefficient,
c_1	–	viscous damping coefficient at higher velocities,
k_0	–	stiffness coefficient at higher velocities,
k_1	–	accumulator stiffness coefficient,

x_0 – initial displacement of a spring with stiffness coefficient k_0.

Recalling to Figure 3 and Eqs. (1) and (2), it is assumed in the Spencer model for fluctuating fields that: parameter α is a linear function of the input voltage with a non-zero initial value at 0 V and viscous damping coefficients c_0 and c_1 are also linear functions of the input voltage. Accordingly, the following functional dependence for the coefficients α, c_0 and c_1 was proposed by Spencer: $\alpha = \alpha(u) = \alpha_a + \alpha_b u$; $c_0 = c_0(u) = c_{0a} + c_{0b} u$; $c_1 = c_1(u) = c_{1a} + c_{1b} u$ where u is the input voltage (applied to the coil).

In the study we assumed that control signal is the input current and damping force is given by Eq. (1) or (2).

4 IDENTIFICATION EXPERIMENT OF AN DAMPER

To prove how the model should reproduce damper behavior we identified the numerical values of the parameters: β, γ, A, k_0, k_1, x_0, α_a, α_b, c_{0a}, c_{0b}, c_{1a}, c_{1b}, y_0, z_0 (we assumed $n = 2$). We conducted a series of RD-1005-3 tests in the experimental setup shown in Figure 4 and thus acquired data for model identification.

We measured force responses under sine, triangular and square displacement excitation with the fixed amplitude of 3×10^{-3} m, frequencies: 1, 2.5, 3.3 and 5 Hz and a programmed sequence of input current variations in the range (0.00, 0.40) A. The data sampling frequency in the tests was 1 kHz. Each test started from the mid-stroke position of the piston. Taking into account the RD-1005-3 applications, the input current in the range (0.00, 0.20) A was of particular interest.

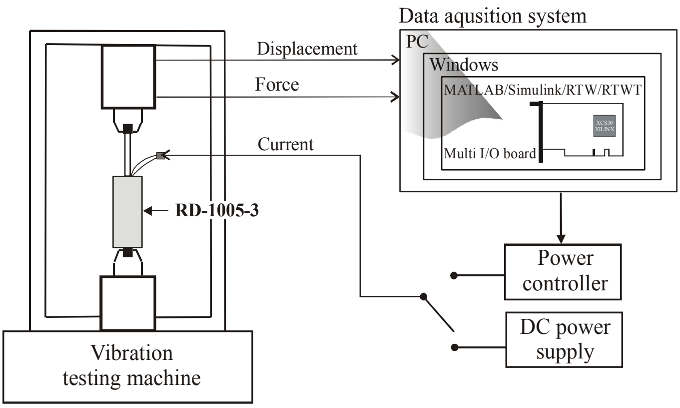

Fig. 4 Diagram of the experimental setup

To illustrate the RD-1005-3 behavior under tested loading conditions we show in Figure 5 force response measured under sine displacement excitation of 1 Hz, 3□10̃3 m and variation of input current as in Figure 6.

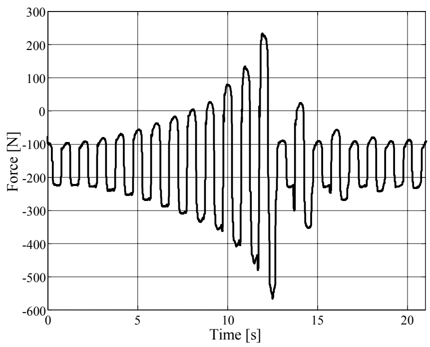

Fig. 5 Force response

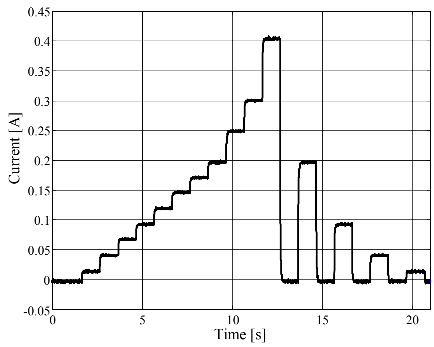

Fig. 6 Variation of input current

In the model identification we employed the constrained nonlinear optimization with the constr procedure available in the optimization toolbox of MATLAB, assuming the quality criterion assumed as of the integral of squared difference between the measured and predicted force responses. Numerical values of the determined model parameters are summarized in Table 1.

Table 1. Parameters of the model

Parameter	Value	Parameter		Value
γ [1/m^2]	77 702.96	c_{0a}	[N·s/m]	557.74
β [1/m^2]	77 449.00	c_{0b}	[N·s/m·A]	3 519.22
A [–]	2 918.55	c_{1a}	[N·s/m]	5 937.07
k_0 [N/m]	3 212.94	c_{1b}	[N·s/m·A]	86 920.99
k_1 [N/m]	468.63	x_0	[m]	0.03
α_a [N/m]	394.03	y_0	[m]	0.00
α_b [N/m·A]	3 772.68	z_0	[m]	0.00

The identified model was used to simulate the RD-1005-3 behaviour under various excitations (sine, triangular and square) and assumed variation of input current. To show how the model fits experimental data Figure 7 provides the measured and predicted force responses obtained for sine displacement and triangular displacement excitations of 1 Hz, 3×10^{-3} m for a programmed sequence of input current variations in the range (0.00, 0.20) A.

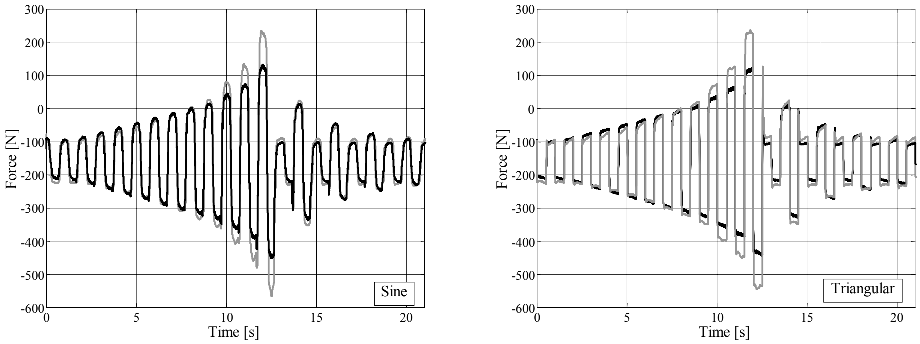

Fig. 7 Measured (▬) and predicted (▬) force responses

In Figure 8 we also show a zoomed section of force responses in time ranges of (1, 11) s and (13, 19) s and variation of input current as in Figure 9. It is apparent that the model portrays RD-1005-3 behaviour in this range with a good fidelity. Similar fidelity was achieved under other displacement excitation, however, for higher input currents the identified model tends to depart from the measurement data.

Generally, the obtained plots reveal that the identified model captures RD-1005-3 behaviour throughout the tested range of loading conditions and input current range (0.00, 0.20) A. Therefore it proves adequate for control design in this range of applied currents.

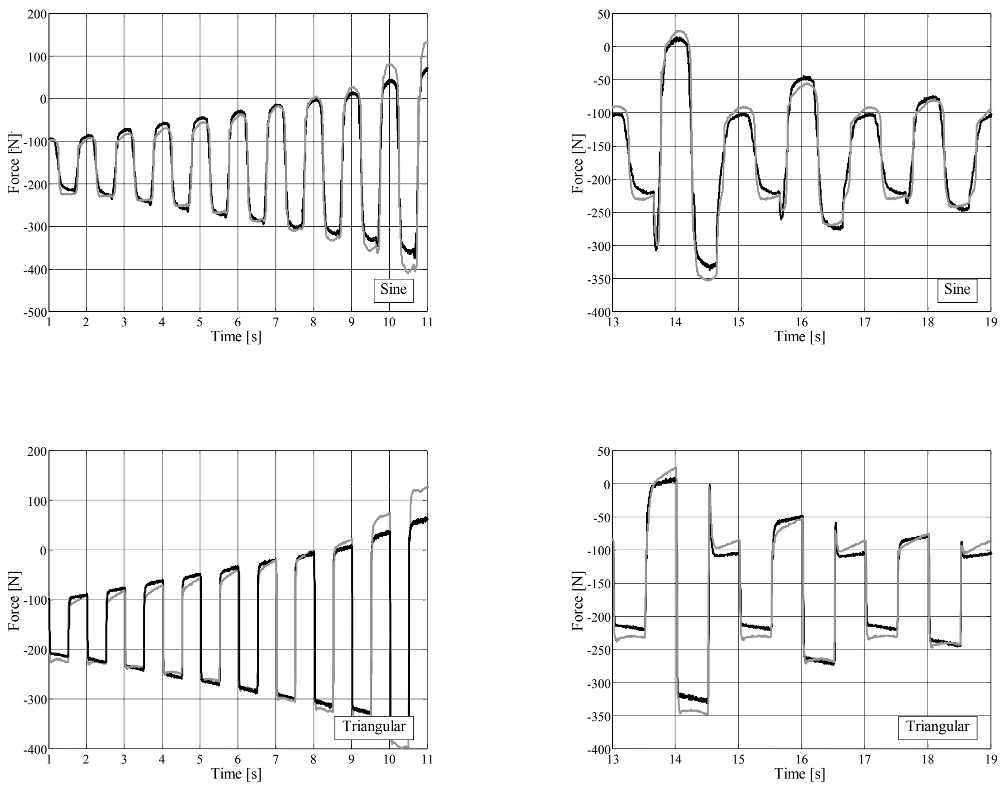

Fig. 8 Zoomed sections of measured (▬) and predicted (▬) force responses

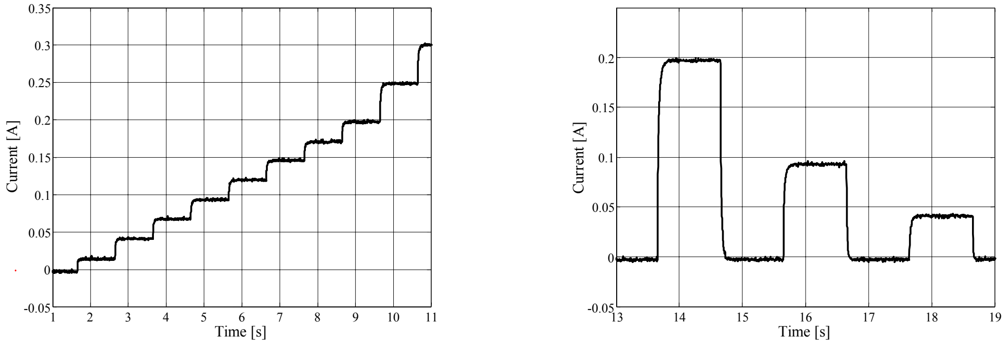

Fig. 9 Zoomed sections of input current variation

5 CONTROL DESIGN

To prove the adequacy of the RD-1005-3 model we investigated a driver's seat with an MR damper which is represented by one-degree-of-freedom system (Fig. 10). The system was tested both numerically and experimentally.

5.1 SIMULATION TESTS

We assume that the system parameters are: mass m=83 kg, stiffness coefficient k=26300 N/m (the natural frequency of the undamped system is f0=2.8 Hz) and the system is base-excited

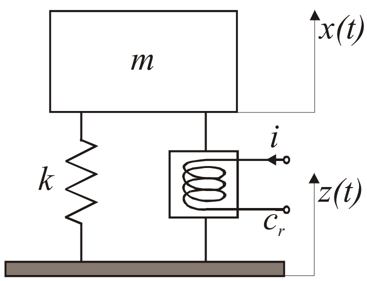

Fig.10 Model of one-degree-of-freedom system with an MR damper

Let us now compare the operating principle of a system with an open loop (where RD-1005-3 operates in the passive mode) and feedback (where RD-1005-3 operates in the controlled mode). In an open-loop system we assumed the input current set to be 0.0 A and 0.1 A. In the feedback system we applied *on-off* algorithm governed by:

$$i = \begin{cases} c_{r1}, & \dot{x}(\dot{x}-\dot{z}) \geq 0 \\ 0, & \dot{x}(\dot{x}-\dot{z}) < 0 \end{cases} \tag{5}$$

where: $x(t)$ − displacement of the mass m, $z(t)$ − displacement of the base, c_r − damping coefficient of an MR damper, i – the input current, c_{r1} was established to be 0.1 A. The constant c_{r1} was derived from simulation tests (Sapiński 2006).

In order to check the adequacy of the operating principle of the *on-off* algorithm the seat was base-exited with sine waves of amplitude 3×10^{-3} m and frequency range (1, 8) Hz. Selected results are shown in Figures 11 and 12. Figure 11 explains the operating principle of the *on-off* algorithm. The plots show time patterns of input and output signals applied in this algorithm which refer to sine base excitation with amplitude 3×10^{-3} m and frequency 3 Hz. The performance for open-loop and feedback systems is compared via acceleration transmissibility plots in Figure 12. It is apparent that for feedback system (controllable damping) we gained both resonant frequency control and high frequency isolation.

The plots in Figures 11 and 12 were derived by simulation with sampling frequency of 4 kHz utilizing the fifth-order numerical procedure (Dormand-Prince method).

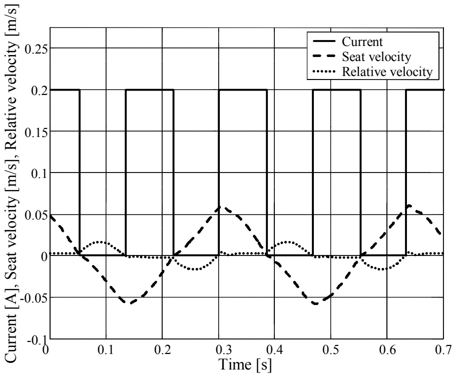

Fig. 11 Input signals and output signal in *on-off* algorithm – simulation

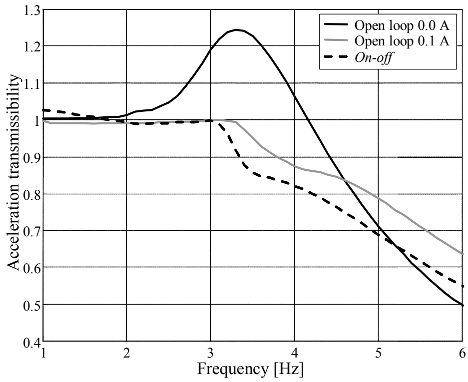

Fig. 12 Acceleration transmissibility – simulation

5.2. EXPERIMENTAL TESTS

The diagram of the experimental setup with a driver's seat is provided in Figure 13. The data acquisition and control system was based on a PC with a multi I/O board installed. The system was supported by MATLAB/Simulink and Real Time Workshop/Real Time Windows Target (RTW/RTWT) running on Windows XP.

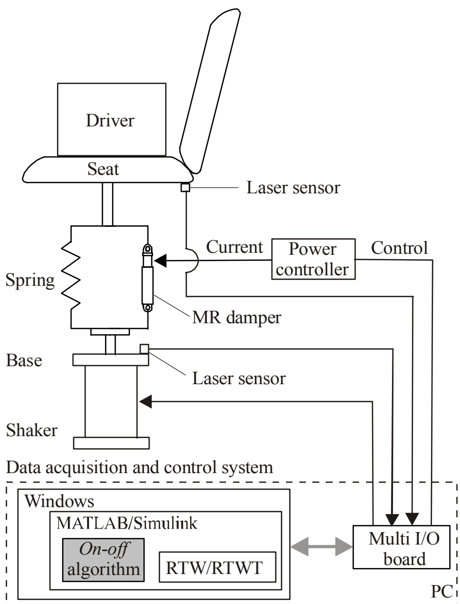

Fig. 13 Diagram of the experimental setup

The seat was equipped with the RD-1005-3 and a specially designed spring with a stiffness coefficient of 26300 N/m. The mass of the seat with driver was set to be 83 kg.

The shaker generating the base excitations was controlled by a PC-multi I/O board system with MATLAB/Simulink support. The shaker base and seat displacements were measured with laser sensors, while velocities and accelerations were reproduced using derivative blocks of Simulink. The damper force was adjusted according to the analog output signal of the multi-channel power controller.

We investigated the system with feedback applying *on-off* algorithm with constant c_{r1} such as that assumed in the simulation tests. First we verified the adequacy of the operating principle of the *on-off* algorithm. Figure 14 shows time patterns of input and output signals applied in the algorithm, measured under sine base excitation with amplitude 3×10^{-3} m and frequency 3 Hz. Next we determined the acceleration transmissibility of the system. Selected acceleration transmissibility plots shown in Figure 15 revealed significant system performance improvements. We gained both best resonant frequency control and superior high frequency isolation. The sampling frequency for real-time tasks was assumed to be 1 kHz.

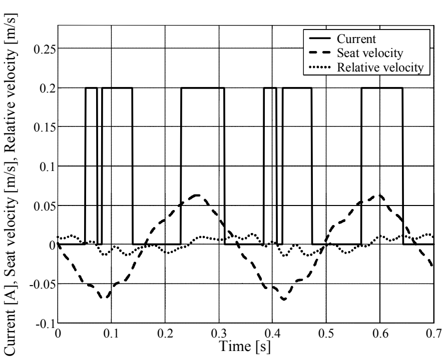

Fig. 14 Input signals and output signal in *on-off* algorithm – measurement

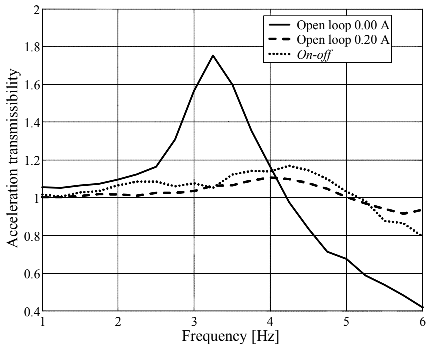

Fig. 15 Acceleration transmissibility – measurement

6 SUMMARY

The model identified allows us to predict RD-1005-3 behavior under fluctuating magnetic fields since its parameters depend on the input current. The determined values of model parameters are valid for the particular RD- 1005-3 used in the tests. Experiments showed that the values of model parameters might vary:

- when the number of working cycles should increase,
- for particular RD-1005-3.

The model identified was applied in control design for an MR damper in a driver's seat. The system was investigated in an open loop and feedback configurations, both numerically and experimentally. In the feedback system we tested on-off control algorithm. The comparison of acceleration transmissibility plots showed that the performance of the feedback system was improved while compared to the open-loop system.

REFERENCES

[1] SAPIŃSKI, B. *Magnetorheological Dampers in Vibration Control*. AGH University of Science and Technology Press, 2006.

[2] SPENCER, B., DYKE, S., SAIN, M. & CARLSON, J. Phenomenological Model of a Magnetorheological Damper. *Journal of Engineering Mechanics*. 1996.

[3] WEN, Y. Method for Random Vibration of Hysteretic Systems. *Journal of the Engineering Mechanics Division*. 1976, pp. 249–263.

[4] http://www.lord.com

ACKNOWLEDGEMENT

The study is supported through the research fund in 2006–2008 as a research grant NO. 4T07C 016 30.

Reviewer: prof. Dr. RNDr. Lubomír Smutný, VŠB - Technical University of Ostrava